



A systematic method for efficient computation of full and subsets Zernike moments

Khalid M. Hosny*

Department of Information Technology, Faculty of Computers and Informatics, Zagazig University, Zagazig, Egypt

ARTICLE INFO

Article history:

Received 29 July 2009

Received in revised form 7 January 2010

Accepted 1 February 2010

Keywords:

Zernike moments
Complex moments
Fast computation
Symmetry property
Gray level images

ABSTRACT

A new method is proposed for fast and accurate computation of Zernike moments. This method presents a novel formula for computing exact Zernike moments by using exact complex moments where the exact values of complex moments are computed by mathematical integration of the monomials over digital image pixels. The proposed method is applicable to compute the full set of Zernike moments as well as the subsets of individual order, repetition and an individual moment. A comparison with other conventional methods is performed. The results show the superiority of the proposed method.

© 2010 Elsevier Inc. All rights reserved.

1. Introduction

Orthogonal circular moments are defined by mapping an image onto a set of orthogonal complex polynomials. Orthogonal moments such as Zernike were first introduced by Teague [26]. According to the orthogonal property, Zernike moments are used to represent an image with the minimum amount of information redundancy [27]. In addition to this essential property, orthogonal Zernike moments are rotational and flipping invariants by nature, while the other kinds of invariance such as translation and scale invariants are achieved through the normalization of their basic polynomials [13]. Due to these characteristics, Zernike moments have been widely used in pattern recognition applications [1,3,28,29], content-based image retrieval [14,17,19], watermarking and data hiding [4,15], biometrics [5,16], edge detection [25], texture analysis [2], image analysis [21] and biomedical engineering [12].

Computational processes of orthogonal moments are time-consuming. Valuable works are proposed in order to efficiently compute different kinds of orthogonal moments [11,23]. Direct computations of Zernike moments through their polynomials are time-consuming. The direct method is impractical in any real world application. Conventional methods for orthogonal Zernike moment's computation produced two types of errors [20]. Consequently, these conventional methods encounter three challenging problems. The optimal method is the one that can overcome or at least minimize the negative effects of these problems.

To tackle the aforementioned problems, there are different groups of existing methods for Zernike moment's computations. In the first group, authors paid their attention to speeding up the computation [6,18,22,24,30]. On the other side, authors paid their attention to increase the accuracy of the computed Zernike moments [7,10].

This paper proposes a systematic method for fast and accurate computation of full and subsets Zernike moment for binary and gray level images. In order to achieve the accuracy, the 2D Zernike moments are exactly computed as a combination of

* Present address: Department of Computer Science, Najran Community College, Najran University, Najran, P.O. Box 1988, Saudi Arabia.
E-mail address: k_hosny@yahoo.com

exact complex moments where the latter are computed exactly by using a mathematical integration of monomials over digital image pixels. The approximation error is completely removed by using the exact computation form. The negative effect of the geometric error is minimized through a proper square to circular transformation where the whole image is completely mapped inside the unit disk. This kind of mapping overcomes the problem of lost information encountered in the conventional methods. To speed up the computation, novel formulae are proposed for systematic and easily programmable computation of the full and subsets of any selected Zernike moments.

Computation of selected subsets of Zernike moments is suitable for the problem of data hiding by using Zernike moments. Selection process of Zernike moments in data hiding is a critical process, where the selected moments must be the most accurate. As discussed in [31], the moments with repetition $q = 4i$ with integer i cannot be computed accurately. Therefore, these moments are not suitable for data hiding. The set S of desirable Zernike moments to be selected for carrying the watermark is $S = \{Z_{pq} : q \leq \text{Max}; q \geq 0; q \neq 4i\}$; where Max is the maximum order of Zernike moments.

Numerical experiments clearly show that the proposed method is an accurate and very fast method. This ensures the superiority of the proposed method over the conventional ones.

The rest of the paper is organized as follows: In Section 2, a brief discussion of Zernike moments and the ZOA approximation computation are given. Section 3 gives an overview of few existing methods for Zernike moment computation. In Section 4, a detailed description of the proposed method is presented. Section 5 is devoted to numerical experiments. Conclusion and concluding remarks are presented in Section 6.

2. Zernike moments

Orthogonal circular Zernike moments are defined by using complex Zernike polynomials. These polynomials are defined inside a unit circle in polar coordinates, where the p -order Zernike polynomial with repetition q is defined as:

$$V_{pq}(r, \theta) = S_{pq}(r)e^{iq\theta} \tag{1}$$

where $\hat{i} = \sqrt{-1}; p = 0, 1, 2, 3, \dots \infty$; the integer q takes positive or zero values according to the conditions $0 \leq q \leq p$ and $(p-q)$ is even. In other words, p is even if q is even and odd if q is odd. Zernike polynomials, $V_{pq}(r, \theta)$, form a complete orthogonal set where their orthogonality relation is defined as follows:

$$\int_0^{2\pi} \int_0^1 V_{nm}(r, \theta)V_{pq}^*(r, \theta)r dr d\theta = \begin{cases} \frac{\pi}{(p+1)}, & p = n, q = m \\ 0, & \text{otherwise} \end{cases} \tag{2}$$

The asterisk symbol $*$ refers to the complex conjugate. The real-valued radial Zernike polynomials $S_{pq}(r)$ are defined as:

$$S_{pq}(r) = \sum_{k=0}^{\frac{p-q}{2}} (-1)^k \frac{(p-k)!}{k!(\frac{p+q}{2}-k)!(\frac{p-q}{2}-k)!} r^{(p-2k)} \tag{3}$$

Like all orthogonal and complete basis, the Zernike polynomials can be used to decompose an analog image intensity function, $f(r, \theta)$, as follows:

$$f(r, \theta) = \sum_{p=0}^{\infty} \sum_{\substack{q=0 \\ p-q=\text{even}}}^p Z_{pq} V_{p,q}(r, \theta) \tag{4}$$

The coefficients Z_{pq} are called 2D Zernike moments of order p and repetition q and defined in polar coordinates as follows:

$$Z_{pq} = \frac{p+1}{\pi} \int_0^{2\pi} \int_0^1 V_{pq}^*(r, \theta)f(r, \theta)r dr d\theta \tag{5}$$

Zernike moments with negative values of q could be obtained by using the relation $Z_{p,-q} = Z_{p,q}^*$. Since the summation to infinity is impossible in computing community, Zernike moments of maximum order equal to Max can be considered where the image intensity function is approximated as follows:

$$\hat{f}_{\text{Max}}(r, \theta) \approx \sum_{p=0}^{\text{Max}} \sum_{\substack{q=0 \\ p-q=\text{even}}}^p Z_{pq} V_{p,q}(r, \theta), \tag{6}$$

The total number of Zernike moments used to reconstruct an image is defined by:

$$N_{\text{Total}} = \begin{cases} (\frac{\text{Max}+2}{2})^2, & \text{Max is even} \\ (\frac{\text{Max}+1}{2})^2 + (\frac{\text{Max}+1}{2}), & \text{Max is odd} \end{cases} \tag{7}$$

The image reconstruction from orthogonal moments only adds the individual components of each order to generate the reconstructed image. Low order moments are employed as global descriptors while in many cases, high order moments are

required to represent the fine details of the image/object. Recently, Zernike moments have been employed in the area of molecular computational biology for comparing small molecules, macromolecules, and protein binding baskets.

Eq. (6) could be rewritten in a form to reconstruct image intensity function by using the expansion with only real-valued functions as follows [13]:

$$\hat{f}_{Max}(x, y) \approx \frac{R_{p0}}{2} S_{p0}(r) + \sum_{p=1}^{Max} \sum_{\substack{q=0 \\ p-q=even}}^p (R_{pq} \cos(q\theta) + I_{pq} \sin(q\theta)) S_{pq}(r) \tag{8}$$

where R_{pq} and I_{pq} are the real and imaginary parts of complex Zernike moments Z_{pq} and defined as:

$$R_{pq} = 2\text{Re}(Z_{pq}) \tag{9.1}$$

$$I_{pq} = -2\text{Im}(Z_{pq}) \tag{9.2}$$

Zernike moments are by nature rotational invariants where their magnitude values are unaffected and remain the same for original and rotated images. Assume that the superscript "Rot" refers to a counterclockwise rotation by angle α . If the original image function is $f(r, \theta)$ and the rotated one is $f^{Rot}(r, \theta - \alpha)$, then we can write $Z_{p,q}^{Rot} = e^{-iq\alpha} Z_{p,q}$. Since the value $|e^{-iq\alpha}| = 1$, the magnitude values of Zernike before and after image rotation are identical.

2.1. Approximate computation of Zernike moments

Computation of Zernike moments by using Eq. (5) is impossible where Zernike polynomials are defined in terms of polar coordinates (r, θ) over a unit disk while the image intensity function is always defined in Cartesian coordinates (x, y) . Consequently, a transformation approach must be defined to overcome this inconsistent problem. Zernike polynomials are converted to be defined in the Cartesian coordinates where the image is transformed to be defined in the same domain. The square image is mapped onto the unit disk as depicted in Fig. 1 where the center of the image is the coordinate origin. For a digital image of size $N \times M$, the transformed coordinates are written as:

$$r_{ij} = \sqrt{\left(\frac{2i - N + 1}{N - 1}\right)^2 + \left(\frac{2j - M + 1}{M - 1}\right)^2} \tag{10}$$

$$\theta_{ij} = \tan^{-1} \left(\frac{(2j - M + 1)/(M - 1)}{(2i - N + 1)/(N - 1)} \right) \tag{11}$$

with $i = 0, 1, 2, \dots, N - 1$; $j = 0, 1, 2, \dots, M - 1$ and $0 \leq r_{ij} \leq 1$. Approximate Zernike moments are direct results of replacing integrals with summations. To compute Zernike moments of discrete-version of the image intensity function, the integrals in Eq. (5) are replaced by summations and the image is normalized inside the unit disk by using image mapping transformation. Based on the principles of mathematical analysis, summations are equivalent to integrals only as the number of sampling points reached infinity. Therefore, the numerical error increases as the number of sampling points decreases. Also, this error increased as the order of moments increased where numerical instabilities are encountered. The zeroth-order approximate (ZOA) Zernike moments of an image size $N \times M$ are [20]:

$$\tilde{Z}_{pq} = \frac{p + 1}{\lambda_p} \sum_{i=0}^{N-1} \sum_{j=0}^{M-1} S_{pq}(r_{ij}) e^{-iq\theta_{ij}} f(i, j) \tag{12}$$

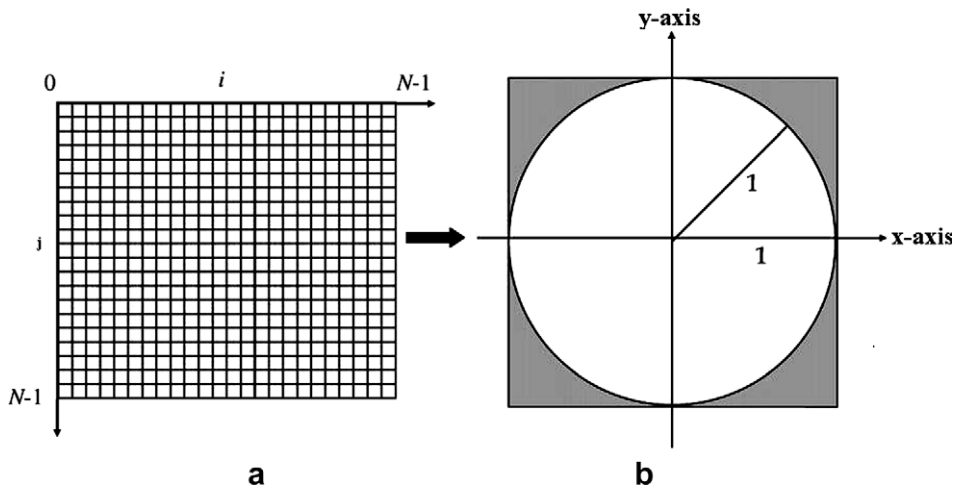


Fig. 1. (a) Image plane. (b) The square image is mapped onto the unit disk.

where λ_p is the total number of pixels that achieve the condition $|r_{ij}| \leq 1$. This number is usually less than the total number of pixels of original image where all pixels with radius greater than the unity are ignored. Eq. (12) is not a very accurate approximation of Eq. (5).

3. Previous methods for computing zernike moments

In this section, a quick review of the previously published methods for computing Zernike moments is presented. A number of works concentrate on speeding up the computation of real-valued radial Zernike function. Kintner [18], Prata and Rusch [24] have proposed recurrence relations for fast computation of radial polynomials of Zernike moments. Chong et al. [6] modified Kintner method to be applicable for all cases of order p and repetition q . Wee et al. [30] have proposed a hybrid method that combines a simplified Kintner's method and other existing methods. Unfortunately, all of these methods are not fast enough and compute Zernike moments approximately by using the ZOA approximation formula in Eq. (12).

3.1. Direct method

The direct method is very time-consuming where computing Zernike moments by using Eq. (12) required the evaluation of the real-valued radial polynomials defined by Eq. (3). This method required four factorial calculations for every real-valued radial polynomial $S_{pq}(r)$. In addition to very long elapsed CPU times, approximated Zernike moments suffer from numerical instabilities where the numerical errors are accumulated. Chong et al. [6] clearly show that, it is necessary to develop new methods for avoiding numerical instabilities when the image size is large.

3.2. Coefficient method

Real-valued radial polynomials defined by using Eq. (3) could be rewritten in a simple way as follows [6]:

$$S_{pq}(r) = \sum_{\substack{k=q \\ p-k=\text{even}}}^p B_{pqk} r^k \quad (13)$$

The coefficients B_{pqk} of real-valued radial Zernike polynomials are defined as:

$$B_{pqk} = \frac{(-1)^{((p-k)/2)} \left(\frac{p+k}{2}\right)!}{\left(\frac{p-k}{2}\right)! \left(\frac{k+q}{2}\right)! \left(\frac{k-q}{2}\right)!} \quad (14)$$

Instead of the time-consuming computation process of the coefficients B_{pqk} by using Eq. (14), recurrence relations are used to efficiently compute these coefficients as follows:

$$B_{ppp} = 1 \quad (15.1)$$

$$B_{p(q-2)p} = \frac{p+q}{p-q+2} B_{ppp} \quad (15.2)$$

$$B_{pq(k-2)} = -\frac{(k+q)(k-q)}{(p+k)(p-k+2)} B_{pqk} \quad (15.3)$$

It is clear that, the values of coefficients B_{pqk} are image-independent; therefore, it could be pre-computed and stored for further use.

3.3. Kintner's method

Kintner [18] proposed a recurrence relation that uses polynomials with low order p and a fixed repetition q to compute the real-valued radial polynomials $S_{pq}(r)$ as follows:

$$S_{pq}(r) = \frac{(K_2 r^2 + K_3) S_{(p-2)q}(r) + K_4 S_{(p-4)q}(r)}{K_1} \quad (16)$$

where K_1, K_2, K_3 and K_4 are defined as:

$$K_1 = \frac{(p+q)(p-q)(p-2)}{2} \quad (17.1)$$

$$K_2 = 2p(p-1)(p-2) \quad (17.2)$$

$$K_3 = -q^2(p-1) - p(p-1)(p-2) \quad (17.3)$$

$$K_4 = -\frac{p(p+q-2)(p-q-2)}{2} \quad (17.4)$$

As discussed previously, Kintner's method cannot be applied in cases where $p = q$ and $p - q = 2$. For these two cases, the direct method is used. This is a weak point where more time demands are added which degrades the efficiency of this method. Chong et al. [6] proposed a modification for Kintner's method and called it the modified kintner. Instead of using the direct method, they proposed the following relations to overcome Kintner's special case limitations:

$$S_{p,p}(r) = r^p, \quad p = q \tag{18}$$

$$S_{(p+2),p}(r) = (p + 2)S_{(p+2),(p+2)}(r) - (p + 1)S_{p,p}(r), \quad p - q = 2 \tag{19}$$

Wee et al. [30] presents what is called simplified Kintner's method. This method requires multiplications and additions processes less than that of the original and modified version proposed in [6]. The simplified Kintner's method uses Eqs. (18) and (19) in addition to the following relations:

$$S_{pq}(r) = (M_1r^2 + M_2)S_{(p-2)q}(r) + M_3S_{(p-4)q}(r) \tag{20}$$

where the coefficients M_1 , M_2 and M_3 are defined as:

$$M_1 = \frac{4p(p - 1)}{(p + q)(p - q)} \tag{21.1}$$

$$M_2 = -\frac{2(p - 1)(p^2 - 2p + q^2)}{(p + q)(p - q)(p - 2)} \tag{21.2}$$

$$M_3 = -\frac{p(p + q - 2)(p - q - 2)}{(p + q)(p - q)(p - 2)} \tag{21.3}$$

3.4. q-Recursive method

Chong et al. [6] proposed a new method for fast computation of real-valued radial polynomials of order p and a repetition q by using three recurrence relations. The first relation is employed for $p = q$. The second relation with the first one is used to compute the radial polynomials with $(p - q) = 2$. The third relation is used to compute the rest of all radial polynomials. These relations are:

$$S_{p,p}(r) = r^p \tag{22}$$

$$S_{p,(p-2)}(r) = pS_{p,p}(r) - (p - 1)S_{(p-2),(p-2)} \tag{23}$$

$$S_{p,(q-4)}(r) = L_1S_{p,q}(r) + \left(L_2 + \frac{L_3}{r^2} \right) S_{p,(q-2)}(r) \tag{24}$$

where L_1, L_2, L_3 and L_4 are defined as:

$$L_3 = -\frac{4(q - 2)(q - 3)}{(p + q - 2)(p - q + 4)} \tag{25.1}$$

$$L_2 = (q - 2) + \frac{L_3(p - q + 2)(p + q)}{4(q - 1)} \tag{25.2}$$

$$L_1 = \frac{q(q - 1)}{2} - qL_2 + \frac{L_3(p + q + 2)(p - q)}{8} \tag{25.3}$$

3.5. Hybrid method

Wee et al. [30] proposed a hybrid method for fast computation of real-valued radial polynomials of order p and repetition q . This method is applicable for fast computation of full set and subsets of Zernike moments. In fact, the full set of radial polynomials is computed by using the fusion of four different relations. Eq. (18) is implemented in the case of $p = q$. Eq. (19) is used to compute the radial polynomials where $p - q = 2$. For $q = 0$ and the value of p starting from 4, the modified Kintner's method is applied. The rest of the radial polynomials are computed by using Prata's relation [24]:

$$S_{p,q}(r) = \left(\frac{2rp}{p + q} \right) S_{(p-1),(q-1)}(r) - \left(\frac{p - q}{p + q} \right) S_{(p-2),q}(r) \tag{26}$$

4. The proposed method

A digital image of size $N \times M$ is an array of pixels. The centers of these pixels are the points (x_i, y_j) , where the image intensity function is defined as shown in Fig. 2a. A circular to square mapping method is applied as shown in Fig. 2b where the whole image is mapped inside the unit disk. The transformed image is defined in the square $[-1/\sqrt{2}, 1/\sqrt{2}] \times [-1/\sqrt{2}, 1/\sqrt{2}]$. The transformed image coordinates are defined as:

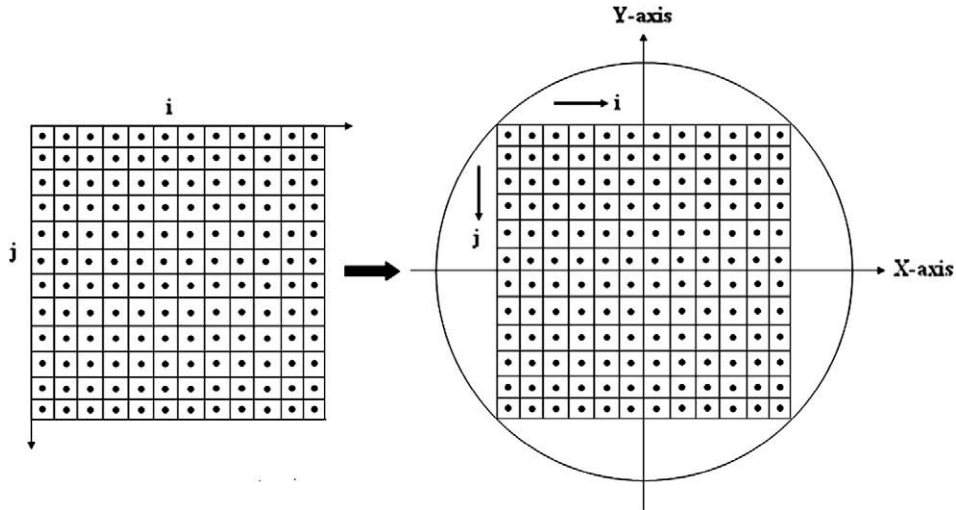


Fig. 2. (a) Digital image with intensity function defined at center of pixels. (b) Mapping of the digital image inside the unit circle.

$$x_i = \frac{2i - N - 1}{N\sqrt{2}}, \quad y_j = \frac{2j - M - 1}{M\sqrt{2}} \tag{27}$$

$$r_{ij} = \sqrt{x_i^2 + y_j^2}, \quad \theta_{ij} = \tan^{-1}(y_j/x_i) \tag{28}$$

with $i = 1, 2, \dots, N$ and $j = 1, 2, \dots, M$. The transformed sampling intervals are:

$$\Delta x_i = \sqrt{2}/N, \quad \Delta y_j = \sqrt{2}/M \tag{29}$$

4.1. Exact Zernike moments

Zernike moments and the complex moments are related by [27]:

$$Z_{pq} = \frac{p+1}{\pi} \sum_{\substack{k=q \\ p-k=even}}^p B_{pqk} C_{\frac{k-q}{2}, \frac{k+q}{2}} \tag{30}$$

where B_{pqk} refers to the coefficients of Zernike polynomials defined by Eq. (14) and $C_{p,q}$ are the complex moments of order $(p + q)$ defined by Eq. (40). Zernike moments could be easily computed according to the difference between the moment order p and the repetition q as shown in Fig. 3. Eqs. (31)–(34) are examples. Eq. (31) is used to compute Zernike moments when the difference between the order p and the repetition q is zero. For difference equals 2, 4 and 6, Eqs. (32)–(34) handle these cases respectively. This procedure is continuous where the difference increases and reaches its maximum value.

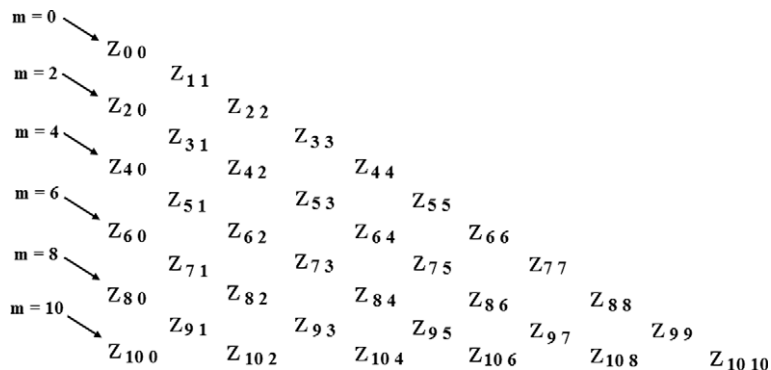


Fig. 3. Zernike moments computed according to the difference “m” between the moment order p and the repetition q .

$$Z_{p,p} = \frac{p+1}{\pi} C_{0,p} \tag{31}$$

$$Z_{p,p-2} = \frac{p+1}{\pi} (B_{p,p-2,p-2} C_{0,p-2} + B_{p,p-2,p} C_{1,p-1}) \tag{32}$$

$$Z_{p,p-4} = \frac{p+1}{\pi} (B_{p,p-4,p-4} C_{0,p-4} + B_{p,p-4,p-2} C_{1,p-3} + B_{p,p-4,p} C_{2,p-2}) \tag{33}$$

$$Z_{p,p-6} = \frac{p+1}{\pi} (B_{p,p-6,p-6} C_{0,p-6} + B_{p,p-6,p-4} C_{1,p-5} + B_{p,p-6,p-2} C_{2,p-4} + B_{p,p-6,p} C_{3,p-3}) \tag{34}$$

The full set of exact Zernike moments with maximum order *Max* are computed by using the following novel formulae:

$$Z_{p,p} = \frac{p+1}{\pi} C_{0,p} \tag{35}$$

$$Z_{p,p-m} = \frac{p+1}{\pi} \sum_{i=0}^{\lfloor \frac{m}{2} \rfloor} B_{p,p-m,p-2i} C_{\frac{m}{2}-i,p-\frac{m}{2}-i} \tag{36}$$

where $p = 0, 1, 2, \dots, Max$; $m \leq p$, $p - m = even$; m is an integer starting with 2 and increases with step 2. The maximum value of m is *Max*. The value of the operator $\lfloor \frac{m}{2} \rfloor$ equal to $(m - 1)/2$ if m is odd; otherwise is equal to $m/2$. The following pseudo-code is applied for computing the full set of Zernike moments by using the proposed method.

```

for p = 0 : 1: Max
    Zp,p = ((p + 1)/pi) * C0,p;
endfor
for m = 2 : 2: Max
    for p = m : 1: Max
        Compute Zp,p-m using Eq. (36);
    endfor
endfor

```

Pseudo-code for computing full set of Zernike moments

Through the next subsections we demonstrate how Eqs. (35) and (36) are adapted to compute different special cases.

4.1.1. Subset Zernike moments of selected order

Zernike moments of a selected order represent a subset of the full set of Zernike moments. For a specific order $p_s = 10$, the subset Zernike moments for this selected order is $\{Z_{10,0}, Z_{10,2}, Z_{10,4}, Z_{10,6}, Z_{10,8}, Z_{10,10}\}$. Subset Zernike moments of the selected order p_s is easily computed as follows:

$$Z_{p_s,p_s-m} = \frac{p_s+1}{\pi} \sum_{i=0}^{\lfloor \frac{m}{2} \rfloor} B_{p_s,p_s-m,p_s-2i} C_{\frac{m}{2}-i,p_s-\frac{m}{2}-i} \tag{37}$$

where m is an integer starting with zero and increases with step 2. The maximum value of m is p_s .

```

read ps;
for m = 0 : 2: ps
    Compute Zps,ps-m using Eq. (37);
endfor

```

Pseudo-code for computing subset of Zernike moments of the selected order p_s

4.1.2. Subset Zernike moments of selected repetition

Zernike moments with a selected repetition represent a subset of the full set of Zernike moments. For a maximum order $Max = 10$, the subset of Zernike moments for a repetition $p_r = 3$ is $\{Z_{3,3}, Z_{5,3}, Z_{7,3}, Z_{9,3}\}$. This subset is easily computed as follows:

$$Z_{p_r+m,p_r} = \frac{p_r+m+1}{\pi} \sum_{i=0}^{\lfloor \frac{m}{2} \rfloor} B_{p_r+m,p_r,p_r+2i} C_{i,p_r+i} \tag{38}$$

where m is an integer starting with 0 and increases with step 2 according to the condition $p_r + m \leq Max$. The following pseudo-code is employed to compute this subset.

```

read pr;
for m = 2 : 2: Max
    if((m + pr) <= Max)
        {
        Compute Zpr + m, pr using Eq. (38);
        m = m + 2;
        }
endfor

```

Pseudo-code for computing a subset of Zernike moments of selected repetition **p_r**

4.1.3. Subset Zernike moments of single moment

A single Zernike moment is a subset of the full set of Zernike moments. To compute a specific single Zernike moment Z_{p_1, p_2} subject to the condition $p_1 - p_2 = \text{even}$; Eq. (36) is rewritten as follows:

$$Z_{p_1, p_2} = \frac{p_1 + 1}{\pi} \sum_{i=0}^{\lfloor \frac{p_1 - p_2}{2} \rfloor} B_{p_1, p_2, p_1 - 2i} C_{\frac{p_1 - p_2}{2} - i, p_1 - \frac{p_1 - p_2}{2} - i} \tag{39}$$

The proposed pseudo-code for computing this subset is written as follows:

```

read p1, p2;
D = p1 - p2;
if (mod (D, 2) == 0) then
    Compute Zp1, p2 using Eq. (39);
else
    Write "There is no Zernike moments for these integers" ;
endif

```

Pseudo-code for computing an individual Zernike moment

4.2. Exact computation of complex moments

Complex moments of order $(p + q)$ for image intensity function $f(x, y)$ are defined as:

$$C_{p, q} = \int_{-\infty}^{\infty} \int_{-\infty}^{\infty} (x + iy)^p (x - iy)^q f(x, y) dx dy, \tag{40}$$

with $\hat{i} = \sqrt{-1}$. By using the binomial theorem, each complex moment can be expressed as a linear combination of geometric moments of the same order or less as follows:

$$C_{p, q} = \sum_{k=0}^p \sum_{j=0}^q \binom{p}{k} \binom{q}{j} (-1)^j i^{k+j} G_{p+q-k-j, k+j} \tag{41}$$

Consequently, exact computation of geometric moments resulting in exact values of complex moments where the geometric moments of order $(p + q)$ for image intensity function $f(x, y)$ are defined as:

$$G_{p, q} = \int_{-\frac{1}{\sqrt{2}}}^{\frac{1}{\sqrt{2}}} \int_{-\frac{1}{\sqrt{2}}}^{\frac{1}{\sqrt{2}}} x^p y^q f(x, y) dx dy \tag{42}$$

Exact values of geometric moments are computed by adapting our previously published methods [8,9].

4.3. Symmetry property of complex moments

For a moment order equal to *Max*, the total number of independent complex moments is $N_1 = (Max + 1)(Max + 2)/2$. Based on the definition of the complex moments in Eq. (40) and the principles of mathematical analysis, we can reduce approximately fifty percent of the computational complexity of complex moments. We can write the following equation:

Table 1
The reduced number of independent complex moments and reduction percentage.

Max	N_1	N_2	Reduction percentage
5	21	12	42.8
10	66	36	45.4
40	861	441	48.7
100	5151	2601	49.5
200	20301	10201	49.75

$$C_{p,q} = C_{q,p}^* \tag{43}$$

Applying Eq. (43) reduces the number of independent complex moments to $N_2 = (N_1/2 + \lfloor Max/2 \rfloor)$ where the reduction percent is $(N_1 - N_2)/N_1$. Table 1 shows the reduced number of independent complex moments and the reduction percentage.

5. Numerical experiments

This section is devoted to numerical experiments that ensure the validity and efficiency of the proposed method. It is divided into three subsections. In the first subsection, a numerical experiment is conducted by using artificial test image. The full set of Zernike moments are computed by using the proposed and ZOA methods. The computed moments are compared with theoretical ones. In the second subsection, reconstruction of real images is considered. MSE and PSNR are commonly used to assess the performance of image reconstruction techniques. Both MSE and PSNR of the proposed and ZOA methods are computed and graphically represented. Finally, numerical experiments are performed to evaluate the computational times. Elapsed CPU times of the proposed method are compared with those corresponding ones of coefficient, modified Kintner, q-recursive and hybrid methods. Based on the extreme computational complexity, the direct method is excluded from our comparison process.

5.1. Artificial test image

Artificial test image is used to prove the validity of the proposed method. A special image with image intensity function $f(x, y) = 1$ for all points (x, y) is considered. The size of this artificial test image is 4×4 . The input image is mapped to be inside the unit circle where the coordinate origin coincides with the center of the circle. The mapped image is defined in the square $[-1/\sqrt{2}, 1/\sqrt{2}] \times [-1/\sqrt{2}, 1/\sqrt{2}]$, where the geometric moments are:

$$G_{pq} = \left(\frac{(1/\sqrt{2})^{p+1} - (-1/\sqrt{2})^{p+1}}{p+1} \right) \left(\frac{(1/\sqrt{2})^{q+1} - (-1/\sqrt{2})^{q+1}}{q+1} \right) \tag{44}$$

Eq. (44) could be rewritten as follows:

$$G_{pq} = \begin{cases} \frac{4(1/\sqrt{2})^{p+q+2}}{(p+1)(q+1)}, & p = \text{even} \\ 0, & p = \text{odd} \end{cases} \tag{45}$$

Substituting Eq. (45) into (41) and (30) yields the theoretical values of Zernike moments. Exact values of Zernike moments are calculated by using Eqs. (35) and (36). The approximated ZOA values are obtained from Eq. (12). It is clear that, the values

Table 2
Theoretical, exact and approximated ZOA Zernike moments for the artificial test image.

p	q	Theoretical, Z_{pq}	Exact, \tilde{Z}_{pq}	ZOA, $\tilde{\tilde{Z}}_{pq}$
0	0	0.6366	0.6366	0.6366
1	1	0	0	0
2	0	-0.6366	-0.6366	-0.7162
2	2	0	0	0
3	1	0	0	0
3	3	0	0	0
4	0	-0.2122	-0.2122	-0.3233
4	2	0	0	0
4	4	-0.2122	-0.2122	0.2114
5	1	0	0	0
5	3	0	0	0
5	5	0	0	0
6	0	0.2122	0.2122	0.3525
6	2	0	0	0
6	4	0.2122	0.2122	0.4026
6	6	0	0	0
7	1	0	0	0
7	3	0	0	0
7	5	0	0	0
7	7	0	0	0
8	0	0.1273	0.1273	0.3642
8	2	0	0	0
8	4	0.1273	0.1273	0.1850
8	6	0	0	0
8	8	0.1273	0.1273	0.1204



Fig. 4. Gray level images: (a) House, (b) baboon, (c) tank, (d) peppers, (e) F16, (f) Lena.

obtained from the proposed method and the theoretical values are identical. For quick comparison, all computed values are shown in Table 2.

5.2. Image reconstruction

Digital images are reconstructed by using two sets of Zernike moments. The first set is computed by using the proposed method while the second set is computed by using the conventional approximation method. For an n -bit image of size $N \times M$, MSE and PSNR are defined as:

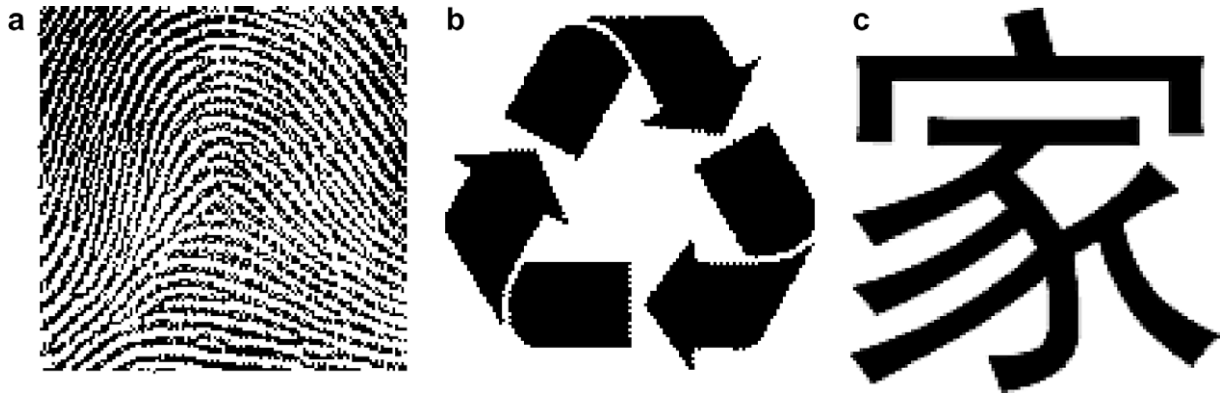


Fig. 5. Binary images: (a) fingerprint, (b) recycle logo, (c) Chinese letter.

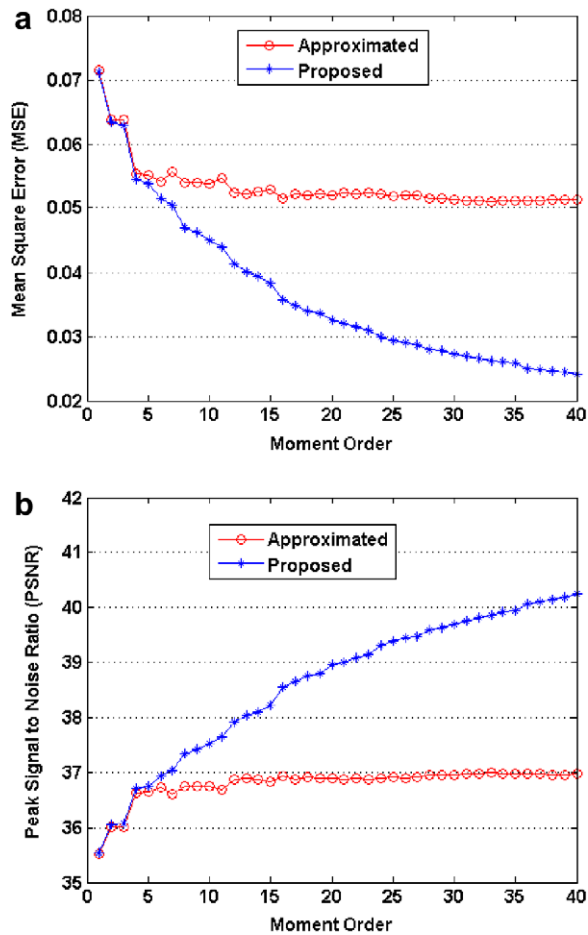


Fig. 6. (a) MSE, (b) PSNR of the house gray level image of size 128×128 .

$$\text{MSE} = \frac{1}{NM} \sum_{i=1}^N \sum_{j=1}^M (\hat{f}_{\text{Max}}(x_i, y_j) - f(x_i, y_j))^2 \quad (46)$$

$$\text{PSNR} = 10 \times \log_{10} \left(\frac{(2^n - 1)}{\text{MSE}} \right) \quad (47)$$

Eq. (46) could be rewritten as follows [20]:

$$\text{MSE} = \sum_{p=0}^{\text{Max}} \sum_{\substack{q \\ p-q=\text{even} \\ q \leq p}} \lambda_p (\hat{Z}_{p,q} - Z_{p,q})^2 + \sum_{p=\text{Max}+1}^{\infty} \sum_{\substack{q \\ p-q=\text{even} \\ q \leq p}} \lambda_p |Z_{p,q}|^2 \quad (48)$$

The first term of Eq. (48) is the discrete approximation error while the second one is the result of using a finite number of moments. The first error increases as *Max* increases while the second error decreases as *Max* increases. The proposed method removes the first error completely. The reconstructed image will be very close to the original one when the maximum moment order reaches a certain value. A numerical experiment is performed where the ‘House’ gray level image of size 128×128 as in Fig. 4a is used with *Max* = 40. Fig. 6a shows MSE for both the proposed and the ZOA method. It is clear that MSE for the proposed method decreases as the moment order increases while it increases as the moment order increases for the approximated method. Fig. 6b shows PSNR for both methods. PSNR for both methods are relatively equal for low order moments. As the moment order increases, the PSNR values are strongly deviated where the values of the proposed method monotonically increase.

5.3. Computational time

Computational time is a very crucial issue. A number of numerical experiments are performed in order to evaluate the performance of the proposed method. The numerical experiments are performed with a computer machine equipped with 1.8 GHz Pentium IV processor and 512 MB RAM. The executed code is designed by using Matlab7.

As described in Section 2, five methods are discussed. Only three of them are compared with the proposed method. The selected three methods were proved to be faster than the others [6,30]. Consequently, we compare the proposed method with the methods of the best performance.

Table 3

Average elapsed CPU times in seconds: full set of Zernike moments for gray level images of size 128×128 .

Moment order	Coefficient method	Kintner method	q_recursive Method	Hybrid method	Proposed Method
Max = 5	0.4210	0.2340	0.2650	0.2340	0.0150
Max = 10	2.0130	0.8120	0.9360	0.8110	0.0310
Max = 15	6.1150	1.7470	1.9970	1.7320	0.0470
Max = 20	13.7590	3.1580	3.5250	3.0140	0.0940
Max = 25	25.6150	4.7580	5.3980	4.7420	0.1880
Max = 30	42.8690	6.8130	7.7850	6.8020	0.3750
Max = 35	66.0180	9.2405	10.5300	9.2350	0.6720
Max = 40	100.3473	13.9531	16.0050	13.8525	0.9380

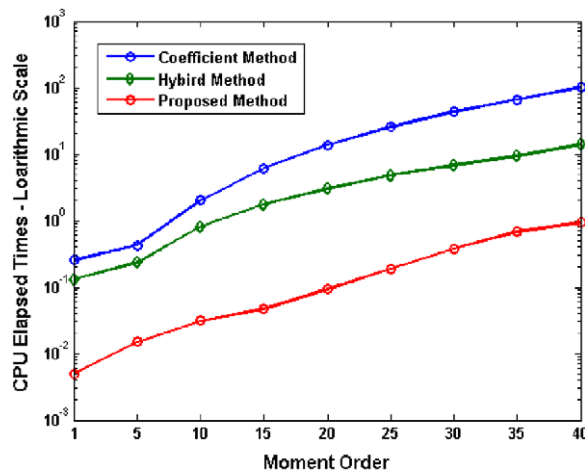


Fig. 7. Elapsed CPU time in seconds. Full set of Zernike moments of gray level images of size 128×128 .

The full set of Zernike moments is computed by using coefficient, modified Kintner, hybrid and proposed methods. In the first experiment, a set of standard gray level images of size 128×128 as displayed in Fig. 4, are used. The average CPU elapsed times for the different aforementioned methods are included in Table 3. It is obvious that CPU elapsed times of modified Kintner and hybrid methods are very close to each other. Therefore, elapsed times of one of them are enough in the comparison process. The average CPU elapsed times of coefficient, hybrid and the proposed methods are plotted against the moment order in Fig. 7. It is clear that, the proposed method has tremendously reduced the execution time.

In the second numerical experiment, the full set of Zernike moments is computed by using the same selected methods. In this experiment, gray level images of size 200×200 are used. The average CPU elapsed times are shown in Table 4. The CPU elapsed times of coefficient, hybrid and the proposed methods are plotted against the moment order in Fig. 8. It is clear that, both the coefficient and hybrid methods are time-consuming. On the other side, the proposed method is very fast.

Another numerical experiment is conducted with a set of binary images of size 128×128 as displayed in Fig. 5. These images are selected from different database sets. Based on the results from the previous numerical experiments, average elapsed CPU times of the selected methods are shown in Table 5. The obtained results clearly show that the performance of the proposed method is much better than the others.

Table 4

Average elapsed CPU times in seconds: full set of Zernike moments for gray level images of size 200×200 .

Moment order	Coefficient method	Kintner method	q_recursive method	Hybrid method	Proposed method
Max = 5	1.0610	0.5460	0.6240	0.5460	0.0310
Max = 10	4.9610	1.9810	2.2470	1.9500	0.0940
Max = 15	15.0700	4.2900	4.8360	4.2430	0.1250
Max = 20	33.8830	7.5190	8.4550	7.4720	0.2190
Max = 25	63.0230	11.6850	13.1040	11.6370	0.3750
Max = 30	106.7190	16.8010	18.7810	16.5670	0.5160
Max = 35	163.9090	22.6820	25.6620	22.4790	0.9690
Max = 40	248.3231	34.4290	38.7492	34.0230	1.2650

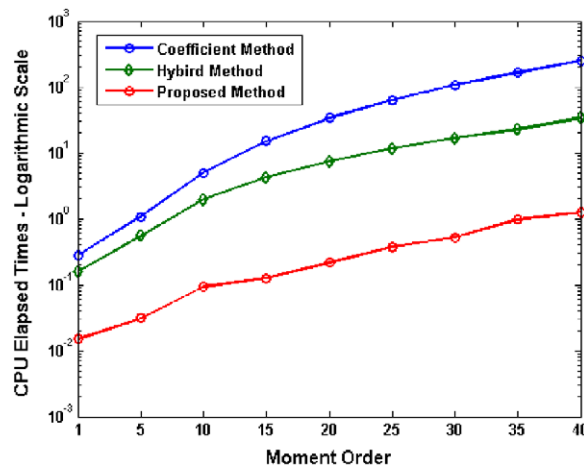


Fig. 8. Elapsed CPU time in seconds. Full set of Zernike moments of gray level images of size 200×200 .

Table 5

Average elapsed CPU times in seconds: full set of Zernike moments for three binary images of size 128×128 .

Moment order	Image of fingerprint		Image of recycle logo		Image of Chinese letter	
	Hybrid method	Proposed method	Hybrid method	Proposed method	Hybrid method	Proposed method
Max = 5	0.641	0.0150	0.4220	0.0110	0.4070	0.0150
Max = 10	2.3590	0.0310	1.1750	0.0160	1.1720	0.0160
Max = 15	3.7660	0.0470	3.3440	0.0400	2.3420	0.0330
Max = 20	5.1250	0.0940	4.8590	0.0780	3.5000	0.0630
Max = 25	6.5780	0.1410	6.6410	0.1103	4.8280	0.1090
Max = 30	8.0000	0.2106	7.9070	0.2018	6.9690	0.2030
Max = 35	9.4220	0.4220	9.3750	0.3170	9.2350	0.2970
Max = 40	10.766	0.6560	10.750	0.5905	10.5203	0.5310

Table 6

Average elapsed CPU times in seconds: full set of Zernike moment by using the proposed method for gray scale images of two different sizes.

	Max = 2	Max = 10	Max = 20	Max = 30	Max = 40	Max = 50	Max = 60	Max = 70
N = 256	0.0470	0.0940	0.2030	0.3750	0.6870	1.1720	2.0150	3.2810
N = 512	0.1100	0.3750	0.7500	1.1720	1.7810	2.5000	3.5940	5.0310

Table 7

Average elapsed CPU times in seconds: subsets of selected Zernike moments for gray level images.

	Coefficient's Method	Kintner's Method	Hybrid Method	Proposed Method
Selected order = 30	2.1400	7.7190	7.3750	0.1870
	8.531	59.1410	48.1720	0.2190
Selected repetition = 12	0.6410	7.3290	7.250	0.1720
	2.360	47.7970	47.5320	0.2030

We must note that, both modified Kintner and Hybrid methods require a very large size of memory for computing and storing the real-valued polynomials $S_{p,q}(x, y)$. Based on the expensive memory requirements, all of these methods are not suitable for large images.

Additional numerical experiments are performed for large images with high order moments. In these numerical experiments, gray level images of size 256×256 and 512×512 are used. The full set of Zernike moments are computed by using the proposed method. Similar to the previous results, the average elapsed CPU times are shown in Table 6. This ensures the superiority of the proposed method where this method requires a very small execution time whatever the size of the input image and the order of the moments are.

Additional numerical experiments are performed in order to compare the elapsed CPU times for computing different subsets of Zernike moments. A subset of selected order equalling 30 is considered. The elapsed CPU times in seconds of the coefficients, modified Kintner, hybrid and the proposed methods are showed in Table 7. This experiment is performed twice, where a gray level image of size 64×64 is used in the first run. The same input image of size 128×128 is used in the second run. It is clear that, the proposed method is very fast method in comparison with the others.

A similar numerical experiment is performed to compute subset Zernike moments of selected repetition equal to 12. The estimated elapsed CPU times are shown in Table 7. This experiment confirms the superiority of the proposed method.

6. Conclusion

A new method is proposed for efficient computation of full and subsets of Zernike moments where novel formulae are proposed to achieve the target. Exact Zernike moments are expressed as a linear combination of exact complex moments. Image reconstruction by using the proposed method shows a great improvement over the conventional methods. The image reconstruction error of the proposed method monotonically decreases as the moment's order increases, while the corresponding error of the conventional methods increases as the moment's order increases. In addition to accuracy advantage of the proposed method, this method is much faster than the conventional methods. In general, the proposed method is outperformed over than all the available methods for Zernike moment computations.

References

- [1] E.M. Arvacheh, H.R. Tizhoosh, Pattern analysis using Zernike moments, IEEE Instrumentation and Measurement Technology Conference, Ottawa, Canada, May 17–19, 2005, pp. 1574–1578.
- [2] V.S. Bharathi, L. Ganesan, Orthogonal moments based texture analysis of CT liver images, Pattern Recognition Letters 29 (13) (2008) 1868–1872.
- [3] A. Broumandnia, J. Shanbehzadeh, Fast Zernike wavelet moments for Farsi character recognition, Image and Vision Computing 25 (2007) 717–726.
- [4] Y. Che, F. Qu, J. Hu, Z. Chen, A geometric robust watermarking algorithm based on DWT-DCT and Zernike moments, Wuhan University Journal of Natural Sciences 13 (6) (2008) 753–758.
- [5] L. Chenhong, L. Zhaoyang, Zernike moment invariants based iris recognition, LNCS 3338 (2004) 554–561.
- [6] C.W. Chong, P. Raveendran, R. Mukundan, A comparative analysis of algorithms for fast computation of Zernike moments, Pattern Recognition 36 (2003) 731–742.
- [7] W. Chong-Yaw, P. Raveendran, In the computational aspects of Zernike moments, Image and Vision Computing 25 (2007) 967–980.
- [8] K.M. Hosny, Exact and fast computation of geometric moments for gray level, Applied Mathematics and Computation 189 (2) (2007) 1214–1222.
- [9] K.M. Hosny, Fast and accurate method for radial moment's computation, Pattern Recognition Letters 31 (2) (2010) 143–150.
- [10] K.M. Hosny, Fast computation of accurate Zernike moments, Journal of Real-Time Image Processing 3 (1–2) (2008) 97–107.
- [11] K.M. Hosny, Exact Legendre moment computation for gray level images, Pattern Recognition 40 (12) (2007) 3597–3605.
- [12] D.R. Iskander, M.J. Collins, B. Davis, Optimal modeling of corneal surfaces with Zernike polynomials, IEEE Transactions on Biomedical Engineering 48 (1) (2001) 87–95.
- [13] A. Khotanzad, Y.H. Hong, Invariant image recognition by Zernike moments, IEEE Transactions on Pattern Analysis and Machine Intelligence 12 (5) (1990) 489–497.
- [14] Y.S. Kim, W.Y. Kim, Content-based trademark retrieval system using visually salient feature, Image and Vision Computing 16 (1998) 931–939.
- [15] H.S. Kim, H.-K. Lee, Image watermark using Zernike moments, IEEE Transactions on Circuits and Systems for Video Technology 13 (8) (2003) 766–775.

- [16] H.-J. Kim, W.-Y. Kim, Eye detection in facial images using Zernike moments with SVM, *ETRI Journal* 30 (2) (2008) 335–337.
- [17] W.C. Kim, J.Y. Song, S.W. Kim, S. Park, Image retrieval model based on weighted visual features determined by relevance feedback, *Information Science* 178 (2) (2008) 4301–4313.
- [18] E.C. Kintner, On the mathematical properties of the Zernike polynomials, *Optica Acta* 23 (8) (1976) 679–680.
- [19] S. Li, M.-C. Lee, C.-M. Pun, Zernike moments features for shape-based image retrieval, *IEEE Transactions on Systems, Man and Cybernetics, Part A* 39 (1) (2009) 227–237.
- [20] S.X. Liao, M. Pawlak, On the accuracy of Zernike moments for image analysis, *IEEE Transactions on Pattern Analysis and Machine Intelligence* 20 (12) (1998) 1358–1364.
- [21] J.A.H. Martin, M. b Santos, J. de Lope, Orthogonal variant moments features in image analysis, *Information Sciences* 180 (6) (2010) 846–860.
- [22] G.A. Papakostas, Y.S. Boutalis, D.A. Karras, B.G. Mertzios, A new class of Zernike moments for computer vision applications, *Information Sciences* 177 (13) (2007) 2802–2819.
- [23] G.A. Papakostas, D.E. Koulouriotis, E.G. Karakasis, A unified methodology for the efficient computation of discrete orthogonal image moments, *Information Sciences* 176 (20) (2009) 3619–3633.
- [24] A. Prata, W.V.T. Rusch, Algorithm for computation of Zernike polynomials expansion coefficients, *Applied Optics* 28 (1989) 749–754.
- [25] Y.-D. Qu, C.-S. Cui, S.-B. Chen, J.-Q. Li, A fast subpixel edge detection method using Sobel–Zernike moments operator, *Image and Vision Computing* 23 (2005) 11–17.
- [26] M.R. Teague, Image analysis via the general theory of moments, *Journal of the Optical Society of America* 70 (8) (1980) 920–930.
- [27] C.H. Teh, R.T. Chin, On image analysis by the method of moments, *IEEE Transactions on Pattern Analysis and Machine Intelligence* 10 (4) (1988) 496–513.
- [28] L. Wang, G. Healey, Using Zernike moments for the illumination and geometry invariant classification of multispectral texture, *IEEE Transactions on Image Processing* 7 (2) (1998) 196–203.
- [29] X.-F. Wang, D.-S. Huang, J.-X. Du, H. Xu, L. Heutte, Classification of plant leaf images with complicated background, *Applied Mathematics and Computation* 205 (2) (2008) 916–926.
- [30] C.Y. Wee, R. Paramesran, F. Takeda, New computational methods for full and subset Zernike moments, *Information Sciences* 159 (2004) 203–220.
- [31] Y. Xin, S. Liao, M. Pawlak, Circularly orthogonal moments for geometrically robust image watermarking, *Pattern Recognition* 40 (12) (2007).